Breakdown of the brain's functional network modularity with awareness

Douglass Godwin[a,1], Robert L. Barry[b,c], and René Marois[a,d,e,1]

[a]Department of Psychology, [d]Vanderbilt Vision Research Center, and [e]Center for Integrative and Cognitive Neuroscience, Vanderbilt University, Nashville, TN 37240; [b]Vanderbilt University Institute of Imaging Science, Vanderbilt University, Nashville, TN 37232; and [c]Department of Radiology and Radiological Sciences, Vanderbilt University Medical Center, Nashville, TN 37232

Edited by Michael S.A. Graziano, Princeton University, Princeton, NJ, and accepted by the Editorial Board February 17, 2015 (received for review July 29, 2014)

Neurobiological theories of awareness propose divergent accounts of the spatial extent of brain changes that support conscious perception. Whereas focal theories posit mostly local regional changes, global theories propose that awareness emerges from the propagation of neural signals across a broad extent of sensory and association cortex. Here we tested the scalar extent of brain changes associated with awareness using graph theoretical analysis applied to functional connectivity data acquired at ultra-high field while subjects performed a simple masked target detection task. We found that awareness of a visual target is associated with a degradation of the modularity of the brain's functional networks brought about by an increase in intermodular functional connectivity. These results provide compelling evidence that awareness is associated with truly global changes in the brain's functional connectivity.

awareness | graph theory | functional connectivity | consciousness

Three broad classes of models have been proposed to explain the neural basis of awareness, with these classes primarily differing on the predicted extent of neural information changes associated with conscious perception. According to focal theories, awareness results from local changes in neural activity in either the perceptual substrates (1–3) or in higher-level nodes of information processing pathways (4). By contrast, network-level theories posit that awareness is tightly associated with activation of parietofrontal attention networks of the brain (5–11). Finally, global models propose that awareness results from widespread changes in the activation state (12–15) and functional connectivity (16–19) of the brain. Though there is strong experimental support for network-level theories, there is scant experimental evidence in favor of truly sweeping, widespread changes in brain activity with conscious perception despite the fact that global scale models have recently come to prominence in the theoretical landscape of this field.

Using a graph theoretical approach applied to ultra-high-field fMRI data, here we experimentally tested a key tenet of global theories: the widespread emergence of large-scale functional connectivity with awareness. Graph theory analyses are ideal tools to test global models of awareness because they can provide concise measures of the integration and segregation of interconnected nodes of a system (20). Applied to functional imaging data, we treat individual brain regions of interest (ROIs) as nodes, functional connectivity between ROIs as edges, and functional brain networks as interconnected modules of nodes. When examining a large set of ROIs that encompass the different networks of the human cerebral cortex (21, 22), we can apply graph theory analyses to estimate the extent to which key measures of global information processing are altered by the state of awareness. This approach has been previously applied to study differences in cognitive states (23–31). Although recent studies have taken advantage of graph theory analysis to examine the connectivity patterns that precede a conscious event (32) or following pharmacologically induced loss of consciousness (33), this approach had yet to be used for characterizing the topology associated with conscious target perception per se, a necessary test for global theories of awareness.

If the changes with awareness are truly global, one should see such changes even if the task does not require complex discrimination, identification, and semantic processes that may recruit vast extents of cortical tissue that are not necessarily associated with conscious perception; in other words, these global changes should appear even for the simple conscious detection of a flashed disk. For this reason, we had participants perform an elementary masked target detection task (Fig. 1) while being scanned at ultra-high field (7 T). The task included three trial types: forward-masked, backward-masked, and no-target conditions. In the forward-masked (paracontrast) condition, a 133-ms-duration annular mask offset 33 ms before the target (a disk whose exterior border coincided with the interior border of the annulus) presented for 33 ms. In the backward-masked (metacontrast) condition, the order of mask/target presentation was reversed while keeping all timing parameters the same. Under such conditions, forward masking of targets has been shown to impair target detection more than backward masking (34, 35). Consequently, the mask/target orderings provided a manipulation of target awareness while maintaining the same mask and target presentation times across both forward- and backward-masked conditions. Because on each trial, participants made a detection response about the presence or absence of the target followed by a confidence rating on their response, subjects' performance could be assessed on both an objective (discriminability index d′) and subjective (confidence rating) measure of awareness (36). In turn, only trials in which the target was either seen (aware) or unseen (unaware) at high confidence levels were used for analysis of brain imaging data. Finally, because the report of the percept was 12 s removed from the stimulus presentations (Fig. 1), the task design

Significance

How the brain begets conscious awareness has been one of the most fundamental and elusive problems in neuroscience, psychology, and philosophy. Correspondingly, this problem has spawned a remarkably large number of theories that differ by the proposed extent of cortical and subcortical changes associated with awareness, ranging from local to global changes in functional connectivity. Graph theoretical techniques, in combination with functional magnetic resonance imaging, provide a well-suited tool to adjudicate between these disparate theories by characterizing whole-brain patterns of communication. In this paper, we demonstrate large-scale differences in functional connections with awareness of a visual target, consistent with global models of awareness.

Author contributions: D.G. and R.M. designed research; D.G. and R.L.B. performed research; D.G. and R.L.B. contributed new reagents/analytic tools; D.G. analyzed data; and D.G. and R.M. wrote the paper.

The authors declare no conflict of interest.

This article is a PNAS Direct Submission. M.S.A.G. is a guest editor invited by the Editorial Board.

[1]To whom correspondence may be addressed. Email: franklin.d.godwin@vanderbilt.edu or rene.marois@vanderbilt.edu.

This article contains supporting information online at www.pnas.org/lookup/suppl/doi:10.1073/pnas.1414466112/-/DCSupplemental.

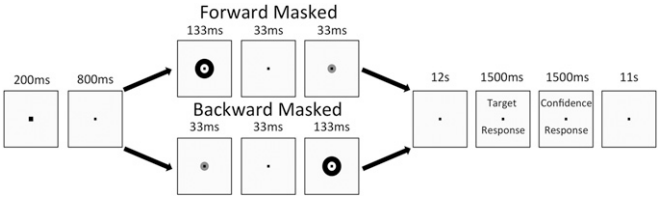

Fig. 1. Schematic of behavioral paradigm with forward-masked and backward-masked trial types (no-target trials not shown). On each trial, participants responded whether they detected the target stimulus and indicated a confidence rating for their answer (*Methods*).

precluded initiation of the motor response itself from influencing estimates of awareness. Although response selection and motor preparation processes likely occur during this period, similar preparation would occur across all conditions.

Results

Target discriminability was greater under the backward-masked condition than the forward-masked condition [main effect of masking condition, $F(1, 92) = 35.51$, $P < 0.001$]. Moreover, this difference in target discriminability between the backward and forward conditions increased at the highest confidence ratings [main effect of confidence rating (Fig. 2), $F(4, 92) = 9.82$, $P < 0.001$]. These results not only demonstrate that the masking manipulation was successful in affecting target detection but also indicate that high confidence ratings provide a robust means of distinguishing between seen and unseen targets.

To assess whether consciously aware and unaware target states were associated with distinct global patterns of functional connectivity, we compared the differences in graph theoretical metrics between seen and unseen trials for high confidence ratings only (ratings of 4 and 5 on a 5-point scale). To increase the number of trials entering into the analysis, each trial type was pooled across both the forward- and backward-masked conditions and classified as target aware (seen) or unaware (unseen) trial types. Because most of the target-aware trials came from the backward-masked condition (~83%), whereas the target-unaware trials primarily originated from the forward-masked condition (~84%), we examined whether the results obtained for the data pooled across masking conditions also held for comparisons within each masking conditions (*SI Results*).

We assessed pairwise functional connectivity across 264 nodes of the cerebral cortex (22) via the generalized psychophysiological interaction (PPI) method (37). The PPI methodology aims to isolate task-induced changes in connectivity from both task-evoked amplitude differences as well as from connectivity differences unrelated to task, using the blood oxygen level-dependent (BOLD) signal (38). Fig. 3*A* illustrates weighted connection matrices for all pairwise PPI parameter estimates, averaged across subjects, between each of the 264 cortical nodes for target aware and unaware conditions organized using the Power et al. (21) parcellation. Projections of the nodes and edges onto 2D cortical representations in Fig. 3*B* highlight the widespread differences in functional PPI strengths between aware and unaware states. It is difficult to draw firm conclusions about connectivity changes with awareness from visual inspection of these matrices or projections alone. Hence, we quantitatively assessed network topology changes with awareness by estimating metrics belonging to key graph theoretical categories of network segregation, integration, and centrality based on the top 10% of connection strengths (Fig. 4*A*), although similar results were obtained using a range of decreased strength thresholds (*SI Results*). If awareness is associated with widespread increases in cortical functional connectivity, it would likely be accompanied by decreased network segregation, increased network integration, and increased node centrality (i.e., highly interactive nodes that facilitate functional integration).

Functional modularity, a measure of the ability to segregate the connectivity patterns into clearly distinct networks, decreased with target awareness [target aware vs. unaware; Wilcoxon's signed-rank test, $P = 0.043$, $PS_{dep} = 0.75$ (a measure of nonparametric effect size)]. Moreover, the average participation coefficient, a value assessing between-network connectivity strengths, was greater in the target aware condition than in the unaware condition (Wilcoxon's signed-rank test, $P = 0.009$, $PS_{dep} = 0.67$). Typically, functional network topologies are complex, with more long-distance connections than lattice (i.e., serially connected) networks but fewer than randomly connected networks (39). This complex topology is thought to be a functionally and metabolically efficient middle ground between random and lattice organizations. Changes in functional modularity and participation toward more random-like (i.e., a normalized value of 1) organizations suggest a shift along this efficiency spectrum to favor longer-distance connections at the expense of segregation of functional networks (26).

Modularity and average participation coefficient were the only metrics to exhibit changes between aware and unaware conditions. The average clustering coefficient, a different measure of network segregation that estimates the degree to which neighboring nodes tend to interconnect with one another, was not affected by the awareness manipulation (Wilcoxon's signed-rank test, $P = 0.689$, $PS_{dep} = 0.54$). The average path length, a metric of integration that measures the average functional distance between two nodes, did not show differences between aware and unaware conditions (Wilcoxon's signed-rank test, $P = 0.753$, $PS_{dep} = 0.54$). Unlike modularity and the participation coefficient, neither of these metrics takes into account module membership. The finding that modularity and participation coefficient—measures that are sensitive to changes in intermodular communication as opposed to changes in individual node connectivity—are those that are altered with awareness strongly suggests that awareness is associated with a breakdown of the brain's network modularity.

The hypothesis that conscious target perception is associated with whole-brain functional connectivity changes would be strongly validated if it were replicated in an independent trial data set: high-confidence false alarms and correct rejections in no-target trials. These two trial types have physically identical stimulus presentations (no targets), but very distinct percepts (aware vs. unaware). False alarm trials showed lower modularity compared with correct rejection trials (Fig. 4*B*; Wilcoxon's signed-rank test, $P = 0.007$, $PS_{dep} = 0.67$), and average participation coefficients were higher during false alarm trials compared with correct rejections as well (Wilcoxon's signed-rank test, $P = 0.0002$, $PS_{dep} = 0.79$). Absent a target, the highly confident awareness of a percept appears sufficient to alter the brain's network topology; this might take place because the false alarm trials correspond to those with structured internal noise sufficient to trigger the simple percept of a flash (40). These results provide converging evidence that reported perception of the target stimulus, regardless of masking manipulations or target presence, produces decreased functional modularity while increasing average participation.

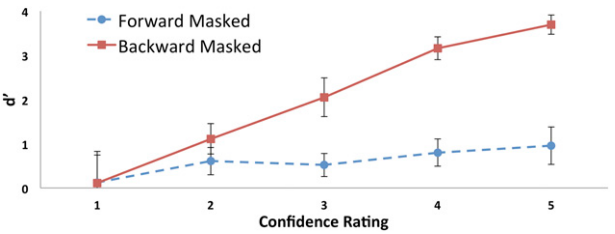

Fig. 2. Behavioral results calculated as d′, a measure of target discriminability from noise. Target stimuli were seen reliably more often in backward-masked trials compared with forward-masked trials, especially at high confidence ratings. Global connectivity analysis was confined to the high-confidence trials (ratings of 4 and 5) to ensure potent differences between aware and unaware states. Error bars show within-group SE.

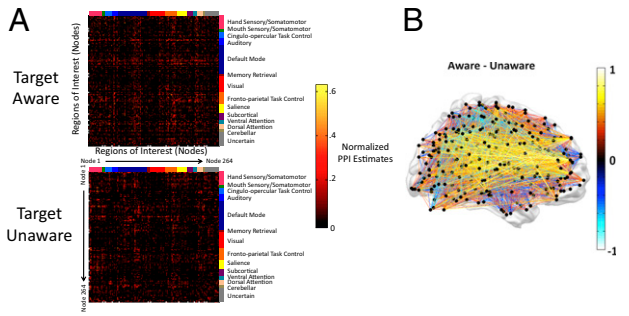

Fig. 3. Group-averaged symmetric connectivity graphs for target-aware and -unaware conditions thresholded at the top 10%. Node coordinates were derived from ref. 21. (*A*) Aware (*Upper*) and unaware (*Lower*) matrices are organized by the 14 network assignments described by Power et al. (21). Heat scale indicates magnitude of interaction regressor (seed × condition; PPI) parameter estimates. (*B*) Differences between subject-averaged connectivity matrices plotted for aware minus unaware. Values were derived by subtracted subject-averaged graphs shown in Fig. 3*A*. Hot colors depict stronger connections for the aware than unaware condition, whereas cool colors depict unaware connections greater than aware. Plots are shown overlaid on a surface projection for reference to anatomical direction and general location. Difference scores with the greatest absolute value are plotted above weaker differences.

It is conceivable that the functional connectivity changes observed with awareness arise from large connectivity changes between a small number of networks, rather than truly global topological changes. If one module or a small set of modules showed greater between-network connectivity changes compared with the others, it should be detectable by testing for an interaction between networks and target awareness state in participation coefficient (a measure of intermodule communication). To test this possibility, we used the fourteen consensus networks identified by Power et al. (21). Using the participation coefficients (calculated either based on module membership detected by our modularity calculations or based on the Power et al. (21) networks as the source of module membership), we estimated the average participation coefficient for nodes in each of the fourteen Power et al. (21) networks for each subject in the target aware and unaware conditions. A repeated-measures ANOVA showed no significant interaction between condition (aware vs. unaware) and network for either of the analytical methods [Fs (13, 299) < 1.03, Ps > 0.43]. It is unlikely that the global modularity and participation differences observed in the present data between the aware and unaware conditions primarily stem from changes in a restricted set of networks.

If not driven by a small number of networks, perhaps our global metrics are instead skewed by massive connectivity changes occurring with awareness in a small number of nodes. To examine this possibility, we tested the integrity of the global network to removal of the most highly interconnected nodes on a per subject basis (20). If these nodes were singularly responsible for what appeared to be global effects, we should no longer observe difference in modularity and participation coefficient between aware and unaware conditions following removal of these highly connected nodes. Excluded nodes were defined as the regions with the greatest summed weighted connection strengths [i.e., the sum of all pairwise connections made by that particular node, thresholded at the top 1% (three nodes) or 10% (27 nodes) of the most interconnected nodes].

Even after removal of these nodes, modularity still differed between aware and unaware, with greater modularity in the unaware compared with aware conditions (1%, $P = 0.046$, $PS_{dep} = 0.71$; 10%, $P = 0.046$, $PS_{dep} = 0.71$). Correspondingly, functional participation still increased with awareness after this targeted attack (1%, $P = 0.01$, $PS_{dep} = 0.67$; marginally at 10%, $P = 0.063$, $PS_{dep} = 0.58$). No significant differences were found for the clustering coefficient (1%, $P = 0.732$, $PS_{dep} = 0.54$; 10%, $P = 0.775$, $PS_{dep} = 0.5$) or average path length (1%, $P = 0.753$, $PS_{dep} = 0.54$; 10%, $P = 0.65$, $PS_{dep} = 0.58$). The effects of awareness on graph theory metrics do not appear to be driven by a small subset of nodes showing the highest connectivity changes.

A final possibility that we considered was that the global connectivity changes were driven by the brain regions that showed significant BOLD amplitude changes with awareness [as identified in statistical parametric maps (SPMs) of the contrast of high-confidence aware vs. high-confidence unaware conditions] (*SI Results*). To address this issue, we performed a similar targeted attack analysis as above, excluding nodes that overlapped with activated voxels in the SPMs. After removal of the eight nodes that were identified as overlapping with foci activated with the awareness manipulation, modularity was still greater in the unaware condition ($P = 0.043$, $PS_{dep} = 0.67$), whereas participation was greater in the aware condition ($P = 0.007$, $PS_{dep} = 0.67$). Again, we found no significant differences between average path length ($P = 0.753$, $PS_{dep} = 0.54$) and the clustering coefficient ($P = 0.797$, $PS_{dep} = 0.5$) between conditions. The brain regions that showed significant BOLD amplitude changes do not solely drive the global connectivity changes observed with the awareness manipulation.

Taken together, these results suggest that target awareness is associated with degradation of modularity in the brain's functional networks via an increase in the participation coefficient without changes in clustering coefficient. Awareness may be associated with a widespread increase in functional connectivity across modules rather than within modules. These results are also in line with reports that manipulations of working memory load can increase intermodular communication and decrease modularity in the absence of global efficiency changes (25), lending credence to our conclusion that decreased functional modularity with awareness results from widespread increased intermodular connectivity.

Discussion

A key finding of the present study is the selective effect of target awareness on a specific subset of graph theory metrics associated with intermodular connectivity. Whereas modularity and intermodular participation indices were affected by the awareness manipulation, there were no changes in clustering coefficient and characteristic path length. Interestingly, the latter two parameters are used to estimate a network's small-worldness

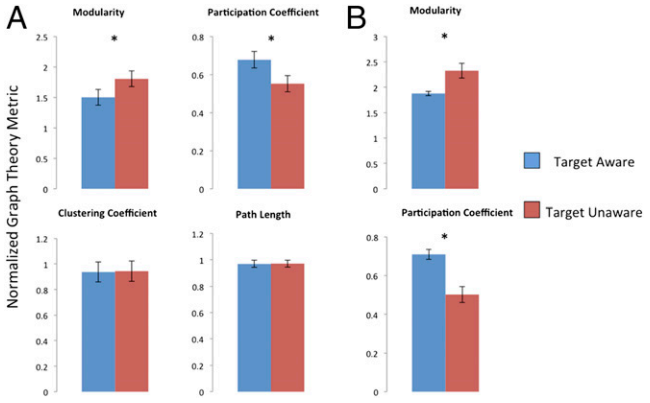

Fig. 4. Effect of awareness manipulation on graph theoretic measurements for target-aware and -unaware trials. (*A*) Comparison of target-aware and -unaware trials (collapsed across target-present conditions). Significant differences between aware vs. unaware conditions were only observed for modularity and participation metrics. (*B*) Comparison of false alarm trials (aware) to correct rejection trials (unaware) from the no-target condition. All *y*-axis values represent the ratio of the observed graph theory metric to the corresponding random graph metrics (*Methods*). Error bars represent within-group SE. Asterisks indicate significant differences between groups at $P < 0.05$.

(41), i.e., a network's tendency to exhibit both high functional segregation and efficiency. The average path length (and the related global efficiency metric) is largely insensitive to multiple, long paths in larger networks (42), precisely the pattern of connections that appear to be most affected by awareness based on participation differences observed in our data. Additionally, existence of small-worldness is defined by strong local clustering (43) that may not be affected by the cross-modular changes seen here with awareness. Awareness of a simple percept may not significantly affect small-worldness because both of the measures used to compute this network feature are more sensitive to intramodular local connections, whereas it is the intermodular connections that are evidently preferentially affected by conscious target perception. As previous studies have identified broad increases in long-distance oscillatory synchrony as a marker of consciousness (33, 44–46), it is conceivable that increase in participation and breakdown of modularity are a result of changes in long-distance functional synchrony following target awareness.

As a whole, the present findings provide strong evidence in support of global theories of awareness, in which the conscious perception of a stimulus is associated with whole-brain dynamic alterations in functional connectivity. Such results may explain why awareness is a unitary phenomenal experience (47), and suggest the means by which information at the focus of attention is broadcasted across the cerebral cortex. It is noteworthy that the changes associated with awareness observed here are more extensive than those reported on the basis of BOLD amplitude changes, which tend to show scattered cortical activation foci with awareness (3, 4, 48–51). Such a BOLD amplitude pattern of frontoparietal activity was in fact observed in our own data when comparing target aware and unaware conditions (*SI Results*). As such, these results imply—aside from differences in sensitivity between BOLD amplitude and functional connectivity approaches—that connectivity differences may reflect latent changes in the functional state of distant brain structures, priming them for target-related activation should the task or environmental situation call upon it.

Importantly, even though our results reveal global summary changes in modularity and participation that are not driven by massive connectivity changes in a single network or small number of nodes, they do not discount focal or network-level contributions to awareness. Instead, we view these global connectivity changes to be a complementary aspect of awareness to the recruitment of frontoparietal regions observed in numerous univariate studies of BOLD amplitude changes (5–11, 48–51). It is only once we are able to integrate the findings obtained at different levels of analysis that we will have a comprehensive understanding of the neural basis of awareness.

Finally, though our findings suggest that changes in a single network do not drive the global functional connectivity changes, not all network interconnectivity is similarly engaged. It may very well be, for example, that visual and auditory awareness would reveal a different balance in functional weights across the brain's networks. Nevertheless, though more studies are evidently required to account for the differentiable aspects of consciousness (52), our results reveal a possible mechanism supporting the integrative nature of this mental state.

Methods

Participants. Twenty-eight individuals (aged 18–33; 15 females) recruited from the Vanderbilt University community participated in the study. All participants had normal or corrected-to-normal vision. The Vanderbilt University Institutional Review Board approved the experimental protocol, and informed consent was obtained from all subjects. Data from four participants were excluded due to technical difficulties (two participants), excessive head motion (>6 mm; one participant), and failure to follow task instructions (one participant).

Behavioral Paradigm. Stimuli were presented using Psychophysics Toolbox extensions (53–55) in MATLAB (MathWorks). All stimuli were shown overlaid on a white background with a persistent, centered, black fixation square (0.25° visual angle). Participants were instructed to monitor each trial for a target stimulus, ignoring a mask stimulus. The target stimulus, a filled gray disk (1° visual angle), was presented at the center of the screen for 33 ms. The mask was a centered, black annulus (from 1° inner edge to 2° outer edge) surrounding the target disk and was shown for 133 ms.

All participants saw three conditions: forward masked, backward masked, and no target. Forward-masked and backward-masked trial types are shown in Fig. 1. In addition, 14 of the 24 participants saw rare oddball images in 5% of all trials. These surprise trials were not analyzed for the current study.

Each trial began with enlargement of the fixation square for 200 ms, cuing the participants for the upcoming target and/or mask presentation 800 ms after the fixation returned to its standard size. An interstimulus interval (ISI) of 33 ms separated the mask and target on all target-present trials. When the mask precedes the target (forward or paracontrast masking) at these timing parameters, target detection is severely impaired. By contrast, when the mask follows the target (backward or metacontrast masking), target detection improves (34, 35). A 12-s fixation interval followed the stimulus presentations to allow the BOLD signal for target detection to be dissociated from the target response BOLD signal (see *fMRI Methods* below). Following the 12-s interval, participants responded to an on-screen prompt (1.5 s) whether they had detected the target stimulus, using one of two right-handed button presses for yes or no. Participants were then prompted (1.5 s) to provide a rating, on a scale of 1–5, of how confident they were in their previous detection response (1 = no confidence; 5 = total confidence) with a left-handed button press. The rating scale remained on screen for the duration of each prompt. The next trial began following another 11-s fixation period.

This stimulus presentation paradigm afforded several advantages for assessing the changes in global functional connectivity with target awareness. First, the reversed mask/target orderings provided a manipulation of target awareness while maintaining identical mask and target presentation durations across both forward- and backward-masked conditions. This consistency across conditions allowed examination of robust effects of target awareness without differences in overall physical stimulation. Moreover, our paradigm yielded robust numbers of trials in which the subjects were highly confident they either did or did not see the target (56). In addition, because all stimuli were presented at fixation, the task required no spatial shifts of attention or eye movements. Finally, by using a very simple stimulus target-mask presentation paradigm that only required rudimentary target stimulus detection (brief percept of a disk), our manipulation provides a strong test of the global theories of awareness because it is unlikely to evoke widespread activation associated with identification, discrimination, or semantic processing (as may occur, e.g., with the attentional blink paradigm).

Twenty-one of the participants completed between four and five fMRI runs (three completed four runs, whereas the remaining 18 completed five runs), each consisting of 20 trials split between the backward-masked, forward-masked, and no-target trials (35%, 35%, and 30%, respectively). Three additional participants completed between five and eight fMRI (one completing five, one completing six, and one completing eight) runs consisting of 15 trials each (five of each of the three trial types). Trial types were presented in a pseudorandomized order in each run. Trials during which participants failed to provide either a detection response or a confidence rating were excluded from analysis (<1% of all trials).

fMRI Methods. Stimuli were presented using an Avotec SV-6011 projector (Avotec, Inc.) back-projected onto a screen inside the scanner. Participants lying in the scanner viewed the screen through a mirror mounted to the head coil. The experiment was performed at the Vanderbilt University Institute of Imaging Sciences on a 7 T Philips Achieva MRI system to benefit from high sensitivity to BOLD signals (57, 58) while providing full-brain coverage at conventional imaging resolutions. Whole-brain, anatomical T1-weighted images were acquired with a $1 \times 1 \times 1$-mm voxel resolution. Functional T2* images were acquired using a 3D PRESTO sequence with $3 \times 3 \times 3$-mm voxels and a 1-s volume acquisition time (59). Scan parameters consisted of a 10-ms repetition time, 14 ms echo time, 10° flip angle, 216 mm × 216-mm in-plane field of view, 72×72 matrix, and 40 slices (covering 120 mm superior–inferior). Each functional scan included either 410 brain volumes (subjects 1–12) or 545 brain volumes (subjects 13–24).

Data preprocessing was performed using Brain Voyager QX 2.3 (Brain Innovation) and included 3D head-motion correction and linear trend removal. Functional and anatomical runs were coregistered and transformed into standard Talairach space (60).

Functional Connectivity Analysis. Cortical ROIs were first defined from the set of coordinates reported in Power et al. (21), in which authors identify nodes based on resting-state connectivity data with strong overlap with known functional-network systems. These nodes were parceled into subgraphs based on community detection algorithms resulting in strong concordance with previously identified functional networks. Coordinates, originally reported

in Montreal Neurological Institute (MNI) space, were converted to Talairach space using the mni2tal.m function in MATLAB. Four-millimeter radius spheres were drawn around each coordinate to create a list of 264 ROIs to serve as nodes for graph theoretical analyses.

To examine connectivity differences associated with target awareness with maximum power, hit trials and miss trials were each collapsed across both forward- and backward-masked trials, yielding a total of 486 high-confidence hit trials and 276 high-confidence miss trials. High-confidence trials were defined as those with ratings of 4 or 5 on the 5-point confidence scale. Given that each condition (hit and miss) was comprised of trials primarily originating from one masking condition (backward and forward, respectively), we also performed the hit vs. miss analyses on high-confidence trials within each masking condition to confirm that the results were not due to masking differences (*SI Methods*). Although the results of this analysis by masking conditions are consistent with the main findings, they suffer from low power because several subjects lacked a sufficient number of high-confidence trials of one trial type to make these comparisons statistically meaningful. Consequently, to further rule out that changes in connectivity differences with awareness may be due to masking differences, we also compared false alarm and correct rejection trials of the no-target condition, because these two trial types are associated with very difference percepts but identical physical presentations.

Task-dependent functional connectivity between nodes was estimated using the generalized psychophysiological interaction (gPPI) method (37). This method aims to account for task-activation effects and non–task-specific correlations separately from task-induced connectivity differences (38). gPPI is considered to be more powerful than a standard PPI analysis (61) and has been shown to be a better estimate of task-based functional connectivity than a cross-correlation coefficient (62) (see *SI Results* for similar results obtained with the Pearson correlations); it uses the general linear model (GLM) with three regressor types: condition-specific task regressors (analogous to those used in standard fMRI GLMs), a "seed" time-course regressor, and condition-specific interaction regressors. The seed time-course regressor is included to capture signal variance in regions that show correlations with the seed region outside of task periods of interest. Interaction regressors were created using the deconvolution method described in McLaren et al. (37) (see *SI Methods* for results without this deconvolution step). In essence, interaction regressors predict correlation with seed region signal, but only during task-relevant time points (capturing an interaction of seed and condition factors). Our GLMs included condition-specific regressors for high- and low-confidence hit trials and miss trials. Each GLM consisted of condition-specific regressors (modeled as events locked to target/mask presentation), a seed node BOLD time course, and condition-specific interaction regressors, all in addition to task regressors of no interest for fixation and response periods. Parameter estimates for high-confidence interaction regressors were recorded and organized for graph theoretical analyses.

A separate GLM was run was for each of the 264 possible seeds for each subject. For each seed region, averaged parameter estimates for PPI interaction regressors were extracted from and averaged across voxels in the 263 remaining ROIs, providing a task-modulated measure of weighted (as opposed to binary) connectivity between each region pair. Larger parameter estimates indicate greater signal coherence between seed and target ROI and thus greater functional connectivity. No directionality was assumed in the data, and reciprocal pairwise connections were averaged to generate the final, symmetric graph. PPI analyses were performed using Brain Voyager QX 2.3 and custom MATLAB software.

Graph Theoretical Analysis. Graph theoretical analyses were performed using the Brain Connectivity Toolbox (41). Graphs (i.e., ROIs and their functional connections) were constructed and analyzed on an individual subject basis for each condition of interest (e.g., high-confidence hit, high-confidence miss trials). As noted in Rubinov and Sporns (41), network properties often differ based on the number of nodes, connections, and degree distribution of a network. To construct network measures that allow comparisons across conditions/graphs that might differ along any of these properties, graph theory metrics are "normalized" by comparing—on a per subject basis—each of these metrics against a null hypothesis network, i.e., a network with a randomized topology that otherwise conserves the size, density, and degree distribution of the original network. All graph theoretic measures were normalized by dividing by their respective, averaged metric calculated across 100 random graphs, generated via the Brain Connectivity Toolbox function randmio_und.m. Statistical significance of normalized graph theoretic measures was performed via Wilcoxon signed-rank tests given the lack of evidence concerning the normal distribution of graph theoretic metrics (20). Because graph theoretic metrics can be threshold dependent (63), it is important to examine graph measurements over a range of possible connection densities. In accordance with prior studies (31, 64, 65), results were obtained for graph density thresholded at the top 10–30% of individual subject connections, with 5% steps, for a total of five threshold levels. Results are presented for the top 10% of connections. Thresholded matrices were rescaled to the range [0, 1] (41). This normalization procedure was calculated by dividing each connectivity value by the maximum value in the graph to rescale values to a similar range as correlations.

Following the approach of previous work in the field, no correction for multiple comparisons across the multiple measures of network properties were applied because of the nonindependence of these measures (31, 41, 66) and because the current study aims only to test the global patterns of topology, rather than the independent properties of individual nodes or ROIs. Correction for multiple comparisons is normally applied when testing several ROIs (33, 67, 68) or if statistical significance (on a per voxel basis) acts as a thresholding step (24, 66, 69–71). The statistical reliability of our findings was provided by a test of replication; the same results were obtained in two independent data analyses: comparisons of hits vs. misses as well as the comparison of false alarms vs. correct rejections.

To measure the graph properties of connections across the brain's neural network with our awareness manipulation, we describe connectivity based on measures of functional segregation, functional integration, and centrality (41). To estimate the functional segregation of the brain's connectivity, we assessed modularity, or the degree to which a graph (i.e., our entire ROI set) can be divided into nonoverlapping modules (i.e., networks of ROIs), via Newman's spectral algorithm for weighted matrices (72). Weighted modularity (Q^w) was calculated by

$$Q^w = \frac{1}{l^w}\sum_{i,j\in N}\left[w_{i,j} - \frac{k_i^w k_j^w}{l^w}\right]\partial_{m_i,m_j},$$

with weighted connections between nodes i and j($w_{i,j}$), sum of all weights in a graph (l^w), weighted degree of a node (k_i), and module containing node i(m_i), and $\partial_{m_i,m_j} = 1$ if $m_i = m_j$.

Based on the modules identified by Newman's algorithm we examined the participation coefficient (y^w), or the degree to which nodes (i.e., ROIs) connect with nodes in other functional modules (networks). Participation provides a measure of centrality per node—i.e., a measure of a node's importance in intermodular communication. Nodes with high participation increase global integration by facilitating between-module communications. The participation coefficient was calculated by

$$y_i^w = 1 - \sum_{m\in M}\left(\frac{k_i^w(m)}{k_i^w}\right)^2,$$

where $k_i^w(m)$ is the weighted degree of connections between node i and nodes in module m.

We additionally measured each node's clustering coefficient, a measure of the degree of segregation present in a network that estimates the extent to which connectivity is clustered around each node irrespective of its module membership. The clustering coefficient (C^w), where t_i is the number of triangles around node I, is calculated with the following formula:

$$C^w = \frac{1}{n}\sum_{i\in N}\frac{2t_i^w}{k_i(k_i-1)}.$$

Finally, average path length (L^w), a measure of network integration, provided a statistic describing the functional distance between nodes, where $d_{i,j}$ is the shortest path length between nodes i and j, computed with a inverse mapping of weight to length.

$$L^w = \frac{1}{n}\sum_{i\in N}\frac{\sum_{j\in N, j\neq i} d_{ij}^w}{n-1}$$

Further descriptions of how these metrics are calculated and their implications can be found in Rubinov and Sporns (41).

As a measure of nonparametric effect size, we report the dependent measures probability of superiority, or PS_{dep} (73). PS_{dep} is defined as

$$PS_{dep} = \frac{n_+}{N},$$

where n_+ is the number of positive difference scores, discarding ties.

ACKNOWLEDGMENTS. This work was supported by National Institutes of Health (NIH) Grant P30-EY008126 to the Vanderbilt Vision Research Center and NIH Grant 5R01EB000461.

1. Moutoussis K, Zeki S (2002) The relationship between cortical activation and perception investigated with invisible stimuli. *Proc Natl Acad Sci USA* 99(14):9527–9532.
2. Zeki S (2008) The disunity of consciousness. *Prog Brain Res* 168:11–18.
3. Tse PU, Martinez-Conde S, Schlegel AA, Macknik SL (2005) Visibility, visual awareness, and visual masking of simple unattended targets are confined to areas in the occipital cortex beyond human V1/V2. *Proc Natl Acad Sci USA* 102(47):17178–17183.
4. Lau HC, Passingham RE (2006) Relative blindsight in normal observers and the neural correlate of visual consciousness. *Proc Natl Acad Sci USA* 103(49):18763–18768.
5. Lumer ED, Friston KJ, Rees G (1998) Neural correlates of perceptual rivalry in the human brain. *Science* 280(5371):1930–1934.
6. Lumer ED, Rees G (1999) Covariation of activity in visual and prefrontal cortex associated with subjective visual perception. *Proc Natl Acad Sci USA* 96(4):1669–1673.
7. Beck DM, Rees G, Frith CD, Lavie N (2001) Neural correlates of change detection and change blindness. *Nat Neurosci* 4(6):645–650.
8. Rees G, Kreiman G, Koch C (2002) Neural correlates of consciousness in humans. *Nat Rev Neurosci* 3(4):261–270.
9. Marois R, Ivanoff J (2005) Capacity limits of information processing in the brain. *Trends Cogn Sci* 9(6):296–305.
10. Naghavi HR, Nyberg L (2005) Common fronto-parietal activity in attention, memory, and consciousness: Shared demands on integration? *Conscious Cogn* 14(2):390–425.
11. Asplund CL, Todd JJ, Snyder AP, Marois R (2010) A central role for the lateral prefrontal cortex in goal-directed and stimulus-driven attention. *Nat Neurosci* 13(4): 507–512.
12. Baars BJ (2002) The conscious access hypothesis: Origins and recent evidence. *Trends Cogn Sci* 6(1):47–52.
13. Baars BJ (2005) Global workspace theory of consciousness: Toward a cognitive neuroscience of human experience. *Prog Brain Res* 150:45–53.
14. Dehaene S, Changeux JP, Naccache L, Sackur J, Sergent C (2006) Conscious, preconscious, and subliminal processing: A testable taxonomy. *Trends Cogn Sci* 10(5): 204–211.
15. Dehaene S, Changeux J-P (2011) Experimental and theoretical approaches to conscious processing. *Neuron* 70(2):200–227.
16. Edelman GM (2003) Naturalizing consciousness: A theoretical framework. *Proc Natl Acad Sci USA* 100(9):5520–5524.
17. van Gaal S, Lamme VAF (2012) Unconscious high-level information processing: Implication for neurobiological theories of consciousness. *Neuroscientist* 18(3):287–301.
18. Tononi G, Sporns O (2003) Measuring information integration. *BMC Neurosci* 4:31.
19. Tononi G (2008) Consciousness as integrated information: A provisional manifesto. *Biol Bull* 215(3):216–242.
20. Bullmore E, Sporns O (2009) Complex brain networks: Graph theoretical analysis of structural and functional systems. *Nat Rev Neurosci* 10(3):186–198.
21. Power JD, et al. (2011) Functional network organization of the human brain. *Neuron* 72(4):665–678.
22. Yeo BT, et al. (2011) The organization of the human cerebral cortex estimated by intrinsic functional connectivity. *J Neurophysiol* 106(3):1125–1165.
23. Ferri R, Rundo F, Bruni O, Terzano MG, Stam CJ (2008) The functional connectivity of different EEG bands moves towards small-world network organization during sleep. *Clin Neurophysiol* 119(9):2026–2036.
24. Bassett DS, et al. (2011) Dynamic reconfiguration of human brain networks during learning. *Proc Natl Acad Sci USA* 108(18):7641–7646.
25. Ginestet CE, Nichols TE, Bullmore ET, Simmons A (2011) Brain network analysis: Separating cost from topology using cost-integration. *PLoS ONE* 6(7):e21570.
26. Kitzbichler MG, Henson RNA, Smith ML, Nathan PJ, Bullmore ET (2011) Cognitive effort drives workspace configuration of human brain functional networks. *J Neurosci* 31(22):8259–8270.
27. Ekman M, Derrfuss J, Tittgemeyer M, Fiebach CJ (2012) Predicting errors from reconfiguration patterns in human brain networks. *Proc Natl Acad Sci USA* 109(41): 16714–16719.
28. Stevens AA, Tappon SC, Garg A, Fair DA (2012) Functional brain network modularity captures inter- and intra-individual variation in working memory capacity. *PLoS ONE* 7(1):e30468.
29. Cole MW, et al. (2013) Multi-task connectivity reveals flexible hubs for adaptive task control. *Nat Neurosci* 16(9):1348–1355.
30. Hermundstad AM, et al. (2013) Structural foundations of resting-state and task-based functional connectivity in the human brain. *Proc Natl Acad Sci USA* 110(15):6169–6174.
31. Cao H, et al. (2014) Test-retest reliability of fMRI-based graph theoretical properties during working memory, emotion processing, and resting state. *Neuroimage* 84: 888–900.
32. Weisz N, et al. (2014) Prestimulus oscillatory power and connectivity patterns predispose conscious somatosensory perception. *Proc Natl Acad Sci USA* 111(4):E417–E425.
33. Schröter MS, et al. (2012) Spatiotemporal reconfiguration of large-scale brain functional networks during propofol-induced loss of consciousness. *J Neurosci* 32(37): 12832–12840.
34. Lefton LA, Newman Y (1976) Metacontrast and paracontrast: Both photopic and scotopic luminance levels yield monotones. *Bull Psychon Soc* 8(6):435–438.
35. Schiller PH, Smith MC (1966) Detection in metacontrast. *J Exp Psychol* 71(1):32–39.
36. Seth AK, Dienes Z, Cleeremans A, Overgaard M, Pessoa L (2008) Measuring consciousness: Relating behavioural and neurophysiological approaches. *Trends Cogn Sci* 12(8):314–321.
37. McLaren DG, Ries ML, Xu G, Johnson SC (2012) A generalized form of context-dependent psychophysiological interactions (gPPI): A comparison to standard approaches. *Neuroimage* 61(4):1277–1286.
38. Gitelman DR, Penny WD, Ashburner J, Friston KJ (2003) Modeling regional and psychophysiologic interactions in fMRI: The importance of hemodynamic deconvolution. *Neuroimage* 19(1):200–207.
39. Bullmore E, Sporns O (2012) The economy of brain network organization. *Nat Rev Neurosci* 13(5):336–349.
40. Ress D, Heeger DJ (2003) Neuronal correlates of perception in early visual cortex. *Nat Neurosci* 6(4):414–420.
41. Rubinov M, Sporns O (2010) Complex network measures of brain connectivity: Uses and interpretations. *Neuroimage* 52(3):1059–1069.
42. Estrada E, Hatano N (2008) Communicability in complex networks. *Phys Rev E Stat Nonlin Soft Matter Phys* 77(3 Pt 2):036111.
43. Humphries MD, Gurney K (2008) Network 'small-world-ness': A quantitative method for determining canonical network equivalence. *PLoS ONE* 3(4):e0002051.
44. Gross J, et al. (2004) Modulation of long-range neural synchrony reflects temporal limitations of visual attention in humans. *Proc Natl Acad Sci USA* 101(35):13050–13055.
45. King JR, et al. (2013) Information sharing in the brain indexes consciousness in noncommunicative patients. *Curr Biol* 23(19):1914–1919.
46. Melloni L, et al. (2007) Synchronization of neural activity across cortical areas correlates with conscious perception. *J Neurosci* 27(11):2858–2865.
47. Seth AK, Izhikevich E, Reeke GN, Edelman GM (2006) Theories and measures of consciousness: An extended framework. *Proc Natl Acad Sci USA* 103(28):10799–10804.
48. Marois R, Leung HC, Gore JC (2000) A stimulus-driven approach to object identity and location processing in the human brain. *Neuron* 25(3):717–728.
49. Haynes JD, Driver J, Rees G (2005) Visibility reflects dynamic changes of effective connectivity between V1 and fusiform cortex. *Neuron* 46(5):811–821.
50. Dehaene S, et al. (2001) Cerebral mechanisms of word masking and unconscious repetition priming. *Nat Neurosci* 4(7):752–758.
51. Marois R, Yi DJ, Chun MM (2004) The neural fate of consciously perceived and missed events in the attentional blink. *Neuron* 41(3):465–472.
52. Tononi G, Edelman GM (1998) Consciousness and complexity. *Science* 282(5395): 1846–1851.
53. Brainard DH (1997) The Psychophysics Toolbox. *Spat Vis* 10(4):433–436.
54. Pelli DG (1997) The VideoToolbox software for visual psychophysics: Transforming numbers into movies. *Spat Vis* 10(4):437–442.
55. Kleiner M, Brainard D, Pelli D (2007) What's new in Psychtoolbox-3. *Perception* 36(14): 1. (abstr).
56. Kunimoto C, Miller J, Pashler H (2001) Confidence and accuracy of near-threshold discrimination responses. *Conscious Cogn* 10(3):294–340.
57. Ogawa S, et al. (1993) Functional brain mapping by blood oxygenation level-dependent contrast magnetic resonance imaging. A comparison of signal characteristics with a biophysical model. *Biophys J* 64(3):803–812.
58. Gati JS, Menon RS, Ugurbil K, Rutt BK (1997) Experimental determination of the BOLD field strength dependence in vessels and tissue. *Magn Reson Med* 38(2):296–302.
59. Barry RL, Strother SC, Gatenby JC, Gore JC (2011) Data-driven optimization and evaluation of 2D EPI and 3D PRESTO for BOLD fMRI at 7 Tesla: I. Focal coverage. *Neuroimage* 55(3):1034–1043.
60. Talairach J, Tournoux P (1988) *Co-Planar Stereotaxic Atlas of the Human Brain. 3-D Proportional System: An Approach to Cerebral Imaging* (Thieme, Stuttgart).
61. Cisler JM, Bush K, Steele JS (2014) A comparison of statistical methods for detecting context-modulated functional connectivity in fMRI. *Neuroimage* 84:1042–1052.
62. Kim J, Horwitz B (2008) Investigating the neural basis for fMRI-based functional connectivity in a blocked design: Application to interregional correlations and psycho-physiological interactions. *Magn Reson Imaging* 26(5):583–593.
63. van Wijk BCM, Stam CJ, Daffertshofer A (2010) Comparing brain networks of different size and connectivity density using graph theory. *PLoS ONE* 5(10):e13701.
64. Dosenbach NUF, Fair DA, Cohen AL, Schlaggar BL, Petersen SE (2008) A dual-networks architecture of top-down control. *Trends Cogn Sci* 12(3):99–105.
65. Rubinov M, et al. (2009) Small-world properties of nonlinear brain activity in schizophrenia. *Hum Brain Mapp* 30(2):403–416.
66. Rubinov M, Sporns O (2011) Weight-conserving characterization of complex functional brain networks. *Neuroimage* 56(4):2068–2079.
67. Bassett DS, Nelson BG, Mueller BA, Camchong J, Lim KO (2012) Altered resting state complexity in schizophrenia. *Neuroimage* 59(3):2196–2207.
68. Lynall ME, et al. (2010) Functional connectivity and brain networks in schizophrenia. *J Neurosci* 30(28):9477–9487.
69. Dosenbach NUF, et al. (2007) Distinct brain networks for adaptive and stable task control in humans. *Proc Natl Acad Sci USA* 104(26):11073–11078.
70. Bassett DS, et al. (2009) Cognitive fitness of cost-efficient brain functional networks. *Proc Natl Acad Sci USA* 106(28):11747–11752.
71. Cole MW, Bassett DS, Power JD, Braver TS, Petersen SE (2014) Intrinsic and task-evoked network architectures of the human brain. *Neuron* 83(1):238–251.
72. Newman ME (2004) Analysis of weighted networks. *Phys Rev E Stat Nonlin Soft Matter Phys* 70(5 Pt 2):056131.
73. Grissom RJ, Kim JJ (2012) *Effect Sizes for Research: Univariate and Multivariate Applications* (Routledge, London).